

Raman Response in Antiferromagnetic Two-Leg $S = \frac{1}{2}$ Heisenberg Ladders

Kai P. Schmidt, Christian Knetter and Götz S. Uhrig

Institut für Theoretische Physik, Universität zu Köln, Zùlpicher Str. 77, D-50937 Köln, Germany

(March 26, 2018)

The Raman response in the antiferromagnetic 2-leg $S = 1/2$ Heisenberg ladder is calculated for various couplings by continuous unitary transformations. For leg couplings above 80% of the rung coupling a characteristic 2-peak structure occurs with a point of zero intensity within the continuum. Experimental data for CaV_2O_5 and $\text{La}_y\text{Ca}_{14-y}\text{Cu}_{24}\text{O}_{41}$ are analyzed and the coupling constants are determined. Evidence is found that the Heisenberg model is not sufficient to describe cuprate ladders. We argue that a cyclic exchange term is the appropriate extension.

PACS numbers: 75.40.Gb, 75.50.Ee, 75.10.Jm

Strongly correlated electron systems in low dimensions are of fundamental interest due to their fascinating properties resulting from strong quantum fluctuations [1–3]. Important experimental insight is gained from spectroscopic measurements of such systems. The spectral densities measured yield information on the kinetics and on the interaction of the elementary excitations as well as on the matrix elements involved. Thus quantitative theoretical calculations of spectral densities are a major task in condensed matter physics. We use optimally chosen continuous unitary transformations (CUT) to map complex many-body problems to a tractable few-body problems [4]. This clear concept serves as a perfect basis to compute spectral densities of strongly correlated systems thus establishing a quantitative contact between theory and experiment [5].

We will focus on optical investigations, in particular on the Raman response, of antiferromagnetic 2-leg Heisenberg ladders realizing quasi one-dimensional (1D) strongly correlated systems. There are several experimental realizations of spin ladders like CaV_2O_5 , SrCu_2O_3 and $\text{La}_y\text{Ca}_{14-y}\text{Cu}_{24}\text{O}_{41}$ rendering direct comparison between theory and experiment possible [7–11].

Raman scattering measures excitations with zero change of spin and momentum. Starting at $T = 0$ from the $S = 0$ ground state the singlet excitations at zero momentum are probed. The Raman response in spin ladders was recently calculated by first order perturbation theory for spin ladders [12] and by exact diagonalization [13]. In this work, we present detailed predictions obtained from CUTs using rung triplets as elementary excitations. Our results are not resolution limited because neither finite size effects occur nor artificial broadenings are necessary.

The Hamiltonian for the 2-leg Heisenberg ladder reads

$$H = \sum_i [J_{\parallel} (\mathbf{S}_{1,i}\mathbf{S}_{1,i+1} + \mathbf{S}_{2,i}\mathbf{S}_{2,i+1}) + J_{\perp}\mathbf{S}_{1,i}\mathbf{S}_{2,i}] \quad (1)$$

where $J_{\parallel} > 0$ and $J_{\perp} > 0$ are the leg and rung couplings; the subscript i denotes the rungs and 1, 2 the two legs. At $T = 0$ the Raman response $I(\omega)$ is given by the retarded resolvent

$$I(\omega) = -\pi^{-1}\text{Im} \langle 0 | R^{\dagger}(\omega - H + i\delta)^{-1} R | 0 \rangle . \quad (2)$$

The observables R^{rung} (R^{leg}) for magnetic light scattering in rung-rung (leg-leg) polarization read in leading order [14,15]

$$R^{\text{leg}} = A_0^{\text{leg}} \sum_i (\mathbf{S}_{1,i}\mathbf{S}_{1,i+1} + \mathbf{S}_{2,i}\mathbf{S}_{2,i+1}) \quad (3a)$$

$$R^{\text{rung}} = A_0^{\text{rung}} \sum_i \mathbf{S}_{1,i}\mathbf{S}_{2,i} . \quad (3b)$$

The factors A_0^{leg} and A_0^{rung} depend on the underlying microscopic electronic model. It is beyond the scope of the present work to compute them. Equally, we do not consider resonating Raman excitation processes. Results will be given in units of the factors squared.

Technically, we employ a CUT to map the Hamiltonian H to an effective Hamiltonian H_{eff} which conserves the number of rung-triplets, i.e. $[H_0, H_{\text{eff}}] = 0$ where $H_0 := H|_{J_{\parallel}=0}$ [4–6]. The ground state of H_{eff} is the rung-triplet vacuum. For the response function $I(\omega)$ the observable R is mapped by the same unitary transformation as the Hamiltonian to an effective observable R_{eff} . We implemented the CUT perturbatively in $x := J_{\parallel}/J_{\perp}$ and calculated H_{eff} to high orders (1-triplet terms: 14th, 2-triplet terms: 13th order). The effective observable R_{eff} is computed to order 10 in the 2-triplet sector and to order 7 in the 4-triplet sector. Generally, higher orders make higher accuracy possible. As a rule of thumb, a calculation in order n accounts for hopping or interaction processes extending over a distance of n rungs.

The truncated series gives quantitative results up to $x \approx 0.6$. Using standard extrapolation techniques like Padé approximants and optimized perturbation theory [17,18], the effective operators R_{eff} and H_{eff} can be calculated up to $x \approx 1$ with an uncertainty of about 5%. A qualitative description is obtained for $x \approx 1.2$. The Raman spectral density is calculated as continued fraction by tridiagonalization [19]. Because in 1D asymptotically free particles with quadratic dispersion display square root behavior at the band edges (van-Hove singularities) we use a square root terminator for the continued fraction. Thus neither finite size nor finite resolution affects our results. No divergences occur because a rung cannot be excited twice, i.e. triplets exclude one another.

The relative motion of a pair of triplets corresponds to the dynamics of a particle on a half-infinite chain [21].

Sectors with odd number of triplets are inaccessible by Raman scattering due to the invariance of the two observables $R_{\text{eff}}^{\text{leg}}$ and $R_{\text{eff}}^{\text{rung}}$ with respect to reflection about the centerline of the ladder. Thus only excitations with even number of triplets matter. Therefore the leading contributions to the Raman response come from the 2-triplet and the 4-triplet sector. The total spectral weight (integrated over frequencies and momenta) of these contributions is depicted in Fig. 1 [16]. The 4-triplet sector has a spectral weight I_4 of less than 7% of the spectral weight I_2 of the 2-triplet sector at $x \approx 1$. Hence we focus on the 2-triplet contribution in the sequel.

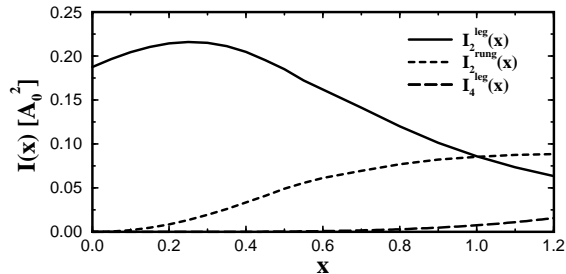


FIG. 1. Spectral weights I_n as function of $x = J_{\parallel}/J_{\perp}$; n denotes the number of triplets involved; the superscript denote the observable as defined in Eq. (3).

In Fig. 2 the spectral density $I(\omega)$ from the 2-triplet sector is shown for various values of $x = J_{\parallel}/J_{\perp}$. The line *shape* is the *same* for R^{rung} and R^{leg} [20] because the Hamiltonian is a weighted sum of the two observables $H = R^{\text{rung}} + xR^{\text{leg}}$ (for $A_0 = 1$). Thus the excited state $R^{\text{rung}}|0\rangle$ equals $-xR^{\text{leg}}|0\rangle$ except for a component proportional to the ground state $|0\rangle$ which does not matter at finite frequencies. This fact leads also to the intersection at $x = 1$ visible in Fig.1.

The spread of the lines in Fig. 2 on increasing x indicates clearly the increasing band width. For small x the Raman intensity shows a strong resonance near the lower band edge. This resonance is a consequence of the 2-triplet attraction on neighboring sites [21,12]. Above a certain finite total momentum this leads to a 2-triplet bound state [21–26,11] of which the resonance at the lower band edge is a precursor. Since for larger x the kinetic energy of the relative motion of the triplets increases the influence of the attraction decreases. Therefore, the resonance is rapidly broadened and shifted to the center of the continuum. In view of analyses of the spin gap [10] we note that it is not possible to detect the onset of the 2-triplet, non-resonant Raman continuum, i.e. twice the spin gap, reliably for $x \gtrsim 0.4$. Furthermore, we found that the non-resonant line shapes do not depend very much on the precise form of the excited state $R|0\rangle$. The qualitative features depend more on kinetics and on interaction.

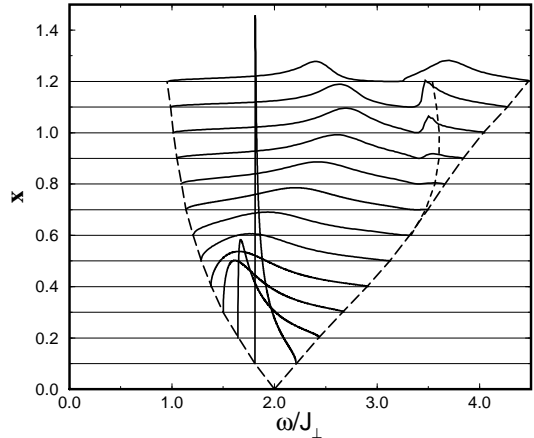


FIG. 2. Raman spectral density $I(\omega)$ for various coupling ratios x . For each curve the total weight is set to $0.1[A_0^2]$. Long dashed lines depict lower and upper band edge of the 2-triplet continuum. The short dashed line shows $2\omega(k=0)$ for $x > 0.5$ where this is *not* the upper band edge ($\omega(k)$ is the 1-triplet dispersion, see inset in Fig. 4).

In Fig. 2 for $x > 0.6$, a second peak is visible near the upper boundary of the 2-triplet continuum, becoming more pronounced on increasing x . This feature is the combined effect of 1-triplet kinetics, 2-triplet interaction and matrix elements. First, the occurrence of a dip in the 1-triplet dispersion $\omega(k)$ at $k = 0$ (cf. inset in Fig. 4) leads to an additional van-Hove singularity situated at $2\omega(0)$ providing additional spectral weight. The importance of this effect is illustrated by the short dashed line in Fig. 2. Second, the additional spectral weight is separated from the main peak by a double zero in the spectral density, see Fig. 2. This double zero stems from a simple zero in the matrix elements implying that at a certain energy ω the state $R|0\rangle$ is orthogonal to the excited state $|\omega\rangle$! This intriguing phenomenon results from destructive interference between several coupling contributions. We found that the destructive interference is triggered by the 2-triplet interaction since it vanishes when the 2-triplet interaction is switched off by hand [27]. Hence the orthogonality is induced by the interaction recalling in a broad sense an orthogonality catastrophe. Indeed, an arbitrarily small amount of the interaction suffices to induce at least a very narrow dip with the double zero at its bottom. We are led to the conclusion that the large density of states provided by the additional van-Hove singularity renders the system particularly susceptible to the interaction-induced orthogonality.

Analyzing experimental data, in Fig. 3 the Raman shift for CaV_2O_5 [8] is shown. This substance is a quasi-2D layered material where the $S = 1/2 \text{ V}^{4+}$ ions form weakly coupled 2-leg ladders (trellis lattice). Susceptibility measurements [28] predict weakly interacting rungs with $x \approx 0.1$. Theoretical analysis in first order yields $x = 0.11$ and $J = 447\text{cm}^{-1}$ [12]. For these values of x

our results can be considered to be exact. It is instructive to compare fits based on our results to the previous analysis. Two fits and their parameters are given in Fig. 3. Assuming the same experimental resolution as in Ref. [12] we find $x = 0.09$ deviating by 20% from the value obtained in first order. A change Δx of order x^2 was to be expected since terms of order x^2 were neglected in the first order analysis [12]. Hence the relative change $\Delta x/x$ is of the order of x . We have to stress that the fits are extremely sensitive to the experimental resolution assumed. Assuming zero resolution ($\Gamma = 0$, see Fig. 3) the best value of x is 0.125, i.e. it is changed by about 40%. This remarkable sensitivity results from the very narrow resonance the height of which changes quickly as function of the resolution. An effective value of Γ adding to the experimental resolution might be generated by residual couplings not considered explicitly. It is unfortunate that the dominant phonon at 940cm^{-1} prevents the observation of the upper part of the continuum so that the theoretically possible high precision analysis cannot be performed. Within the non-resonant Raman theory, our results exclude that the shoulder at 970cm^{-1} besides the dominant phonon is of magnetic origin. We conclude that the previous analyses [28,8,13,12] and ours agree within the achievable accuracy.

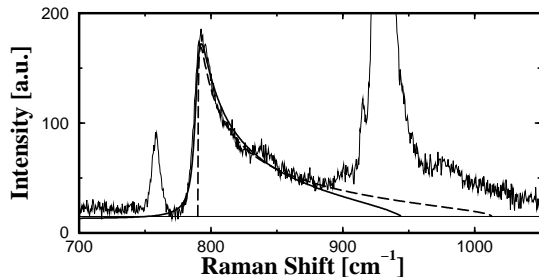


FIG. 3. Raman response for CaV_2O_5 from Ref. [8]. Solid line: fit with $x = 0.09$, $J_\perp = 431\text{cm}^{-1}$ assuming an experimental resolution of $\Gamma = 3\text{cm}^{-1}$. Long dashed line: fit with $x = 0.125$, $J_\perp = 447\text{cm}^{-1}$, $\Gamma = 0$. Thin constant line: offset of the fits to account for background.

In Fig. 4 the Raman lines [10] for $\text{La}_6\text{Ca}_8\text{Cu}_{24}\text{O}_{41}$ are analysed. $\text{La}_6\text{Ca}_8\text{Cu}_{24}\text{O}_{41}$ is a layered material containing CuO_2 1D spin chains and Cu_2O_3 2-leg spin ladders [29]. The inter-ladder coupling is weak and frustrated (trellis lattice) so that the ladders can be treated as isolated ladders. Because the atomic distance between neighboring copper sites in rung and leg direction is almost the same one expects the spin ladders to be in the isotropic regime $x \approx 1$. This view is corroborated by the analysis of the 2-triplet bound state observed by infrared (IR) absorption [11] leading to values of J_\perp between 1020 and 1100cm^{-1} . On the other hand, the spin gap values and neutron scattering data cannot be reconciled with the model in Eq. 1 for $J_\parallel \approx J_\perp$, see e.g. [30] and references therein. Either values of x beyond unity

or extensions of the model are necessary.

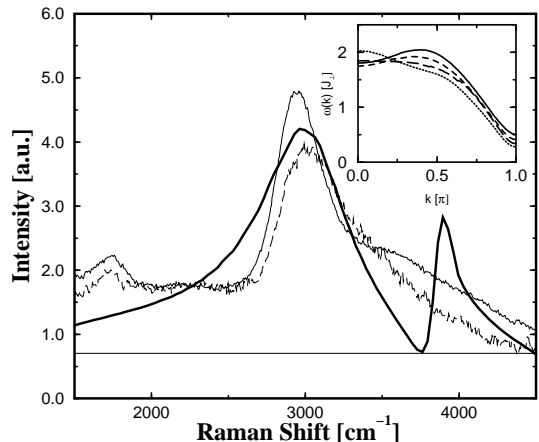


FIG. 4. Raman response for $\text{La}_6\text{Ca}_8\text{Cu}_{24}\text{O}_{41}$. Rough thin lines: experimental data [10] in (aa) (dashed) and (cc) (solid) polarization scaled to the same constant value between 2000 and 2500cm^{-1} . Thick solid line: theory for $J_\parallel = J_\perp = 1100\text{cm}^{-1}$ and resolution $\Gamma = 3\text{cm}^{-1}$. Thin constant line: offset of the fit to account for background. Inset: 1-triplet dispersions $\omega(k)$ for $J_\parallel = J_\perp$ and $x_{\text{cyc}} = 0, 0.05, 0.10, 0.15$ (solid, dashed, long dashed, dotted).

Assuming the model in Eq. 1 and the observables in Eq. 3 the line shapes for the two polarizations should be identical independent of the value of x as explained above. The fact that this is not the case, see Fig. 4, indicates that an extension of the model is necessary though it cannot be excluded that a modification of the observables (3) would also explain the deviations.

The $x = 1$ result agrees quite well with the experimental data. The value $J_\perp = 1100\text{cm}^{-1}$ is consistent with the IR result [11]. The main peak is situated at the right energy and has approximately the right width. The weight of the experimental high energy shoulder corresponds to the weight in the theoretical second peak at higher energies. However, important deviations remain. (i) Experimentally, there is a high energy shoulder but no second peak. (ii) The main experimental peak is sharper. Inspecting Fig. 2 these discrepancies are not remedied by assuming a larger coupling ratio x . Furthermore, the sensitivity on the excited vector $R|0\rangle$ is not very large so that an explanation of the deviations in terms of modifications of the observables R in (3) is unlikely. Hence extensions of the model must indeed be considered.

Numerous results favor the inclusion of a 4-spin cyclic exchange term H_{cyc} as next important term [31–34]. Especially in the spin ladder material $\text{La}_6\text{Ca}_8\text{Cu}_{24}\text{O}_{41}$ about 10% cyclic exchange reconcile results for the spin gap, the dispersion and the weighted spectral densities [30,35,11]. The term H_{cyc} reads

$$H_{\text{cyc}} = 2J_{\text{cyc}} \sum_i [(\mathbf{S}_{1,i}\mathbf{S}_{1,i+1})(\mathbf{S}_{2,i}\mathbf{S}_{2,i+1}) + (\mathbf{S}_{1,i}\mathbf{S}_{2,i})(\mathbf{S}_{1,i+1}\mathbf{S}_{2,i+1}) - (\mathbf{S}_{1,i}\mathbf{S}_{2,i+1})(\mathbf{S}_{1,i+1}\mathbf{S}_{2,i})]. \quad (4)$$

To assess the effect of a cyclic exchange term on the Raman line shape qualitatively we include the 1-triplet dispersion for various values of $x_{\text{cyc}} = J_{\text{cyc}}/J_{\text{perp}}$ in the inset in Fig. 4. The gap $\omega(\pi)$ decreases on increasing x_{cyc} [30]. For $x_{\text{cyc}} = 0.1$ we find $\Delta = 0.337J_{\perp}$ in very good agreement with the result from neutron scattering $\Delta = 0.343J_{\perp}$ [35]. More important for the Raman line shape is that the dip in the dispersion $\omega(k)$ at $k = 0$ is reduced on increasing x_{cyc} . The dispersion is monotonic for $x_{\text{cyc}} = 0.10$. Additionally, preliminary results on the 2-triplet terms show that the attractive interaction between triplets is diminished by the cyclic exchange. Thus we expect the pronounced zero inside the continuum of the Raman line to disappear on inclusion of cyclic exchange leading to an asymmetric broad peak with a shoulder at the high energy side as measured, see Fig. 4 and Refs. [7,9,10]. We estimate that the deviation (i) is remedied by a 4-spin cyclic exchange term with $x_{\text{cyc}} \approx 0.1$ in agreement with other analyses [30,35,11].

The deviation (ii) in the sharpness of the main peak may also be remedied by the inclusion of the 4-spin cyclic exchange term. Alternatively, one might invoke a doping effect, namely holes in the ladder, since the lines are considerably sharper for $\text{Sr}_{14}\text{Cu}_{24}\text{O}_{41}$ [10], in particular in (*cc*) polarization. Other results [11,36], however, show that there are no holes in the ladders shedding doubt on an explanation in terms of holes in the ladders.

In conclusion, we calculated the Raman response in the antiferromagnetic 2-leg $S = 1/2$ Heisenberg ladder in terms of dressed rung-triplets as elementary excitations. Our results are based on a continuous unitary transformation introducing the number of elementary excitations as good quantum number. We demonstrated that the 2-triplet contributions dominate by far. Unexpectedly we found a 2-peak structure composed of a broad main peak and a secondary peak at higher energies for $J_{\parallel} \gtrsim 0.8J_{\perp}$. From the inconsistency with the experimental finding for $\text{La}_6\text{Ca}_8\text{Cu}_{24}\text{O}_{41}$ we infer that the model must be extended for which a 4-spin cyclic exchange term is the best candidate to date. To exclude possible effects due to doping we urge for further investigations in undoped materials such as SrCu_2O_3 .

We gratefully acknowledge M. Grüninger and E. Müller-Hartmann for very helpful discussions and M. Konstantinović for kind provision of experimental data. This work is supported by the DFG in SP1073.

- [3] P.W. Anderson, *Science* **288**, 480 (2000)
- [4] C. Knetter and G.S. Uhrig, *Eur. Phys. J. B* **13**, 209 (2000)
- [5] C. Knetter, K.P. Schmidt, M. Grüninger, and G.S. Uhrig, *cond-mat/0106077*
- [6] C. Knetter, K.P. Schmidt, and G.S. Uhrig, in preparation
- [7] M.V. Abrashev, C. Thomsen, M. Surtchev *Physica C* **280**, 297 (1997)
- [8] M.J. Konstantinović, Z.V. Popović, M. Isobe and Y. Ueda, *Phys. Rev. B* **61**, 15185 (2000)
- [9] Z.V. Popović et al., *Phys. Rev. B* **62**, 4963 (2000)
- [10] S. Sugai and M. Suzuki, *Phys. Stat. Sol. (b)* **215**, 653 (1999)
- [11] M. Windt et al., *Phys. Rev. Lett.* in press, *cond-mat/0103438*
- [12] C. Jurecka, V. Grützun, A. Friedrich, and W. Brenig, *cond-mat/0104465*
- [13] Y. Natsuma, Y. Watabe and T. Suzuki, *Phys. Soc. Japan* **67**, 3314 (1998)
- [14] P.A. Fleury and R. Loudon, *Phys. Rev.* **166**, 514 (1968)
- [15] B.S. Shastry and B.I. Shraiman, *Phys. Rev. Lett.* **65**, 1068 (1990)
- [16] For details on the computation of the spectral weights see Refs. [5,6].
- [17] C. Domb and J.L. Lebowitz, *Phase Transitions and Critical Phenomena*, Academic Press, New York, vol. 13 (1989)
- [18] H. Kleinert, *Path Integrals in Quantum Mechanics, Statistics, and Polymer Physics*, World Scientific, Singapore (1995)
- [19] E.R. Gagliano and C.A. Balseiro, *Phys. Rev. Lett.* **59**, 2999 (1987)
- [20] P.J. Freitas and R.R.P. Singh, *Phys. Rev. B* **62**, 14113 (2000)
- [21] G.S. Uhrig and H.J. Schulz, *Phys. Rev. B* **54**, R9624 (1996); *ibid.* **58**, 2900 (1998)
- [22] O.P. Sushkov and V.N. Kotov, *Phys. Rev. Lett.* **81**, 1941 (1998)
- [23] K. Damle and S. Sachdev, *Phys. Rev. B* **57**, 8307 (1998)
- [24] S. Trebst, H. Monien, C.J. Hamer, Z. Weihong, and R.R.P. Singh, *Phys. Rev. Lett.* **85**, 4373 (2000)
- [25] W. Zheng, C.J. Hamer, R.R.P. Singh and S. Trebst, and H. Monien, *Phys. Rev. B* **63**, 144410 (2001)
- [26] C. Jurecka and W. Brenig, *Phys. Rev. B* **61**, 14307 (2000)
- [27] C. Knetter, K.P. Schmidt, and G.S. Uhrig, submitted to *Physica B*
- [28] D.C. Johnston et al., *cond-mat/0001147*
- [29] E.M. Mc.Carron, M.A. Subramanian, J.C. Calabrese, and R.L. Harlow, *Mater. Res. Bull.* **23**, 1355 (1998)
- [30] S. Brehmer, H.J. Mikeska, M. Müller, N. Nagaosa, and S. Uchida, *Phys. Rev. B* **60**, 329 (1999)
- [31] J.J. Schmidt and Y. Kuramoto, *Physica* **B163**, 443 (1990)
- [32] Y. Honda, Y. Kuramoto, and T. Watanabe, *Phys. Rev. B* **47**, 11329 (1993)
- [33] E. Müller-Hartmann and A. Reischl, *cond-mat/0105392*
- [34] R. Coldea et al., *Phys. Rev. Lett.* **86**, 5377 (2001)
- [35] M. Matsuda, K. Katsumata, R.S. Eccleston, S. Brehmer, and H.J. Mikeska, *J. Appl. Phys.* **87**, 6271 (2000)
- [36] N. Nücker et al., *Phys. Rev. B* **62**, 14384 (2000)

[1] J. Orenstein and A.J. Millis, *Science* **288**, 468 (2000)

[2] S. Sachdev, *Science* **288**, 475 (2000)